# Cross Sections and Charged-Particle Multiplicities at 102 and 405 GeV/$c$

C. Bromberg, D. Chaney, D. Cohen,† T. Ferbel,‡ P. Slattery, and D. Underwood
*University of Rochester, Rochester, New York 14627*

and

J. W. Chapman, J. W. Cooper, N. Green, B. P. Roe, A. A. Seidl, and J. C. Vander Velde
*University of Michigan, Ann Arbor, Michigan 48104*

(Received 16 October 1973)

We have measured the total inelastic cross section ($\sigma_{inel}$) and charged-particle multiplicities obtained in $pp$ collisions at 405 GeV/$c$. The data are from a preliminary 12 000-picture bubble-chamber exposure. We find $\sigma_{inel}=32.8\pm1.0$ mb; the low moments of the multiplicity distribution for negative particles are $\langle n_-\rangle=3.50\pm0.07$, $D_-=2.37\pm0.05$, $f_2^-=2.1\pm0.2$, and $f_3^-=0.1\pm0.9$. We also present updated results at 102 GeV/$c$.

In this Letter we report our latest measurements of topological, elastic, and total cross sections in $pp$ collisions at 102 and 405 GeV/$c$ utilizing the 30-in. Argonne National Laboratory–National Accelerator Laboratory (ANL/NAL) liquid-hydrogen bubble chamber. The 102-GeV/$c$ data are from a 31 000-picture exposure (about 128 events per mb of cross section), while the 405-GeV/$c$ data are from a 12 000 picture exposure (about 65 events per mb of cross section). The present work supersedes a previous publication of preliminary results at 102 GeV/$c$ based on a 5000-picture exposure.[1]

Both exposures were scanned twice for events produced by beamlike tracks; a third comparison scan was performed to adjudicate any inconsistencies in beam counts or event topologies found in the two previous independent scans of the film. The 405-GeV/$c$ data and the initial 102-GeV/$c$ exposure[1] were taken using 70-mm film, while the major fraction of the 102-GeV/$c$ experiment was recorded using 35-mm film, with the chamber operating in a double-pulsing mode. All exposures were divided equally between the University of Michigan and University of Rochester groups and were handled in a similar manner. Scanning at the University of Michigan was performed using projectors having 40× magnification of the image from film to scanning table, while a 25× magnification was used at the University of Rochester.

In Table I we present our measurements of the topological cross sections at 102 GeV/$c$. Corrections to the charged-particle cross sections have been made for Dalitz decays of the $\pi^0$'s.[2] Results from the two scans indicated that the double-scan efficiency for two-pronged events which had proton recoil momenta in excess of 200 MeV/$c$ was $(99\pm1)\%$, while for higher prong numbers it was essentially 100%. A best estimate of the charged-prong count was made for events containing a visible secondary interaction near the vertex (~1% of the total). All apparent odd-pronged events (~0.2% of the total) were classified as belonging to even-pronged topologies of the next-highest–integer value. A small correction, corresponding to a shift in the multiplicity distribution of approximately 10% of that resulting from the Dalitz-pair correction, was also applied to the data to take account of secon-

TABLE I. Topological cross sections at 102 GeV/$c$.

| Prong number | Number observed | Corrected[a] number | Cross[b] section (mb) |
|---|---|---|---|
| 2 | 1266 | 896[c] | 7.0 ±0.4 |
| | | 562[d] | 4.5 ±0.4 |
| 4 | 1000 | 1012 | 7.9 ±0.3 |
| 6 | 955 | 965 | 7.5 ±0.3 |
| 8 | 745 | 743 | 5.8 ±0.2 |
| 10 | 489 | 479 | 3.7 ±0.2 |
| 12 | 218 | 209 | 1.6 ±0.1 |
| 14 | 86 | 79 | 0.62 ±0.07 |
| 16 | 29 | 27 | 0.21 ±0.04 |
| 18 | 7 | 6 | 0.05 ±0.02 |
| 20 | 2 | 2 | 0.016±0.011 |
| Total inelastic | | 4084 | 31.9 ±0.7 |
| Total | 4797 | 4980 | 38.9 ±0.8 |

[a]See text.
[b]The density of hydrogen used in the calculation of cross sections is $0.0630\pm0.0005$ g/cm$^3$ (L. Hyman, private communication).
[c]Elastic.
[d]Inelastic.

dary interactions occurring within 0.5 cm of the main production vertex which might have gone unnoticed. Finally, the two-prong data were corrected for small-angle proton losses (short proton recoils which were not visible in the bubble chamber). The latter loss was determined by fitting the elastic scattering data by an exponential form

$$(d\sigma/dt)_{t=0}\exp(At+Bt^2), \quad (1)$$

where $t$ is the square of the four-momentum transfer from incident to outgoing proton. This form is preferable to a simple exponential fall-off in $t$ when fitting over a range of $t$ values which includes the "break" near $-t\approx 0.1$ GeV$^2$ (Amaldi[3]). The fit was carried out using the unbiased data for $|t|>0.05$ GeV$^2$, with the constraint that the cross section at $t=0$ be given by the lower limit provided by the optical theorem,[3]

$$(d\sigma/dt)_{t=0}=\sigma_T^2/16\pi(\hbar c)^2, \quad (2)$$

where for $\sigma_T$ we used our measured value of the total cross section (iterated with respect to the corrections required for $|t|<0.05$ GeV$^2$).

Figure 1(a) displays the measured elastic differential cross section at 102 GeV/$c$ and the fit of Eq. (1) to the data. The best-fit parameters are given on the graph. The value of $B$ is consistent with recent measurements reported at NAL.[3] The two-prong inelastic cross section was also corrected for slow-proton recoils assuming the same detection efficiency as a function of $t$ as was found using the fit in Fig. 1.

The events appearing in the elastic cross-section data of Fig. 1 were obtained through kinematic fitting of all two-pronged events by the elastic-scattering hypothesis. To ascertain the discrimination of the $\chi^2$ fit to background from reactions of the kind

$$p+p\to p+p+\pi^0, \quad p+p\to p+p+\pi^0+\pi^0, \quad (3)$$

we proceeded as follows: We selected all four-pronged events belonging to the inclusive reaction

$$p+p\to p+\text{anything}, \quad (4)$$

where the final-state proton is slow in the laboratory. These events were converted into fake two-pronged events by ignoring all tracks except for the slow proton and the fastest positive track emerging from the main interaction point. These fake two-prongs were processed through our kinematic fitting programs, and the fraction of events which were fitted by the elastic hypothesis

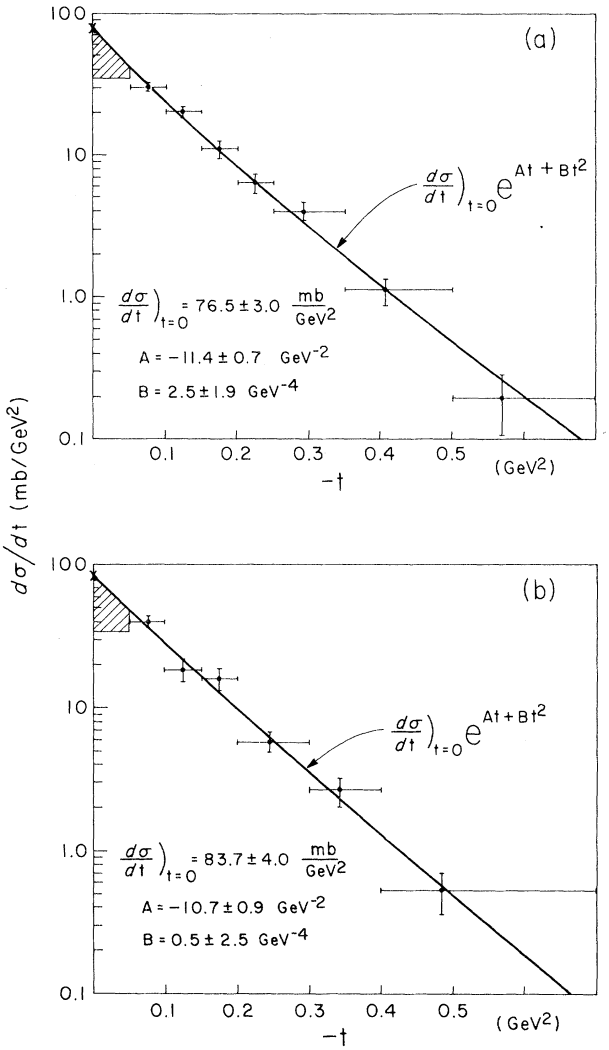


FIG. 1. Differential cross section for elastic scattering events at (a) 102 and (b) 405 GeV/$c$. Shaded area, event losses at small $t$.

provided us with an estimate of the corrections we made to the elastic data from the sort of channels given in Reaction (3). The uncertainty in this fitting procedure is reflected in the errors we assign to the two-prong cross sections. Errors on the $\geq$four-prong cross sections are mainly statistical.

Table II presents, at 405 GeV/$c$, results similar to those given in Table I. In Fig. 1(b) we display the elastic-scattering differential cross section for the higher-energy data. The analysis proceeded in the same fashion as at 102 GeV/$c$. The larger error bars reflect the lower statistics as well as the poorer resolution for the two-pronged inelastic/elastic separation at 405 GeV/c.

TABLE II. Topological cross sections at 405 GeV/$c$.

| Prong number | Number observed | Corrected[a] number | Cross[b] section (mb) |
|---|---|---|---|
| 2 | 600 | 516[c] | 7.8 ±0.7 |
| | | 179[d] | 2.7 ±0.1 |
| 4 | 298 | 303 | 4.6 ±0.3 |
| 6 | 331 | 336 | 5.1 ±0.3 |
| 8 | 370 | 375 | 5.7 ±0.3 |
| 10 | 312 | 313 | 4.7 ±0.3 |
| 12 | 252 | 252 | 3.8 ±0.2 |
| 14 | 190 | 187 | 2.8 ±0.2 |
| 16 | 95 | 89 | 1.3 ±0.1 |
| 18 | 66 | 63 | 0.95 ±0.12 |
| 20 | 40 | 37 | 0.56 ±0.09 |
| 22 | 23 | 21 | 0.32 ±0.07 |
| 24 | 10 | 9 | 0.14 ±0.05 |
| 26 | 3 | 2 | 0.030 ± 0.021 |
| 28 | 1 | 1 | 0.015 ± 0.015 |
| 30 | 2 | 2 | 0.030 ± 0.021 |
| 32 | 1 | 1 | 0.015 ± 0.015 |
| Total inelastic | | 2170 | 32.8 ±1.0 |
| Total | 2594 | 2686 | 40.6 ±1.2 |

[a]See text.

[b]The density of hydrogen used in the calculation of cross sections is 0.0630 ± 0.0005 g/cm$^3$.

[c]Elastic.

[d]Inelastic.

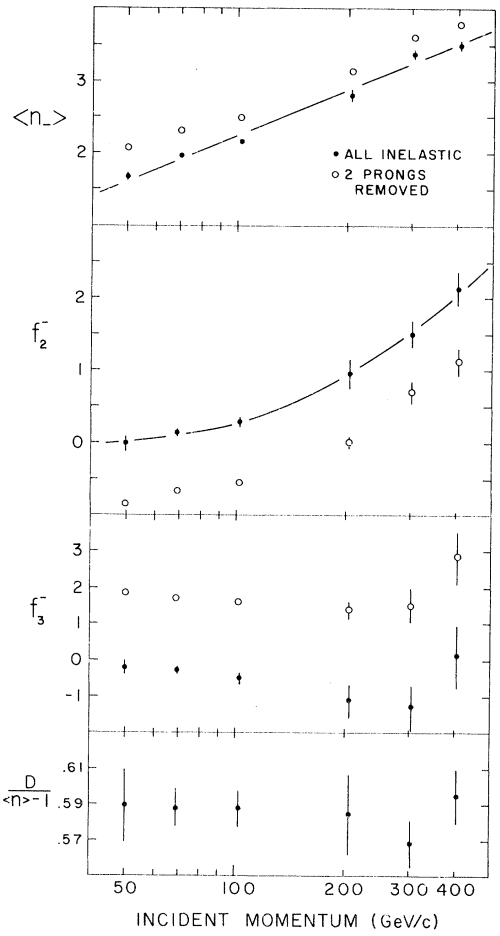


FIG. 2. Negative-particle multiplicity distribution moments and $D/(\langle n\rangle - 1)$ as functions of the incident momentum. The curves are the result of logarithmic fits described in the text.

Table III displays several calculated quantities of interest using the data presented in the previous tables. In Fig. 2 we combine our results with similar previous measurements at energies $\geq$ 50 GeV.[4] We note the following:

(1) The average negative-particle multiplicity in inelastic $pp$ collisions between 50 and 405 GeV/$c$ rises approximately as ln$s$. There is, however, a substantial scatter of the experimen-

TABLE III. Low-order moments of the multiplicity distributions.

| | 102 GeV/$c$ | | 405 GeV/$c$ | |
|---|---|---|---|---|
| | All charged | Negative charge | All charged | Negative charge |
| $\langle n\rangle$ | 6.32 ± 0.07 | 2.16 ± 0.04 | 8.99 ± 0.14 | 3.50 ± 0.07 |
| $D$ | 3.13 ± 0.04 | 1.56 ± 0.02 | 4.75 ± 0.09 | 2.37 ± 0.05 |
| $\langle n\rangle/D$ | 2.02 ± 0.03 | 1.38 ± 0.03 | 1.89 ± 0.05 | 1.47 ± 0.04 |
| $\langle(n-\langle n\rangle)^3\rangle/D^{3a}$ | 0.65 ± 0.04 | | 0.75 ± 0.07 | |
| $\langle(n-\langle n\rangle)^4\rangle/D^{4a}$ | 3.16 ± 0.13 | | 3.62 ± 0.28 | |
| $f_2$ | 3.45 ± 0.25 | 0.28 ± 0.07 | 13.5 ± 0.9 | 2.1 ± 0.2 |
| $f_3$ | 3. ± 1. | − 0.50 ± 0.15 | 30. ± 8. | 0.1 ± 0.9 |
| $f_4$ | − 34. ± 7. | 0.00 ± 0.34 | 30. ± 100. | 1. ± 4. |

[a]The skewness $[\langle(n-\langle n\rangle)^3\rangle/D^3]$ and the kurtosis $[\langle(n-\langle n\rangle)^4\rangle/D^4]$ are identical for the total and negative-charged-particle multiplicity distributions. $D^2 = \langle(n-\langle n\rangle)^2\rangle$ is the variance of the multiplicity distribution. For definition of the $f$ moments see Ref. 5.

tal points from a smooth rise with $s$; this is true for all the inelastic data as well as for multiplicities excluding the two-pronged topology, thus suggesting the presence of interesting structure or additional systematic uncertainties in these experiments. The best-fit linear dependence of $\langle n_- \rangle$ on ln$s$ is $\langle n_- \rangle = -2.5 + 0.9 \ln s$. We do not quote errors on these parameters because of the poor quality of the fit (an additional quadratic term does not substantially improve the fit).

(2) The $f_2^-$ moment[5] requires a $(\ln s)^2$ term in addition to a ln$s$ term to obtain an acceptable $\chi^2$ for its energy dependence:

$$f_2^- = (8.5 \pm 3.5) + (-3.8 \pm 1.3) \ln s + (0.43 \pm 0.12)(\ln s)^2.$$

(3) The errors on $f_3^-$ are presently too large to allow discrimination between linear and quadratic dependences on ln$s$.

(4) The value of $D/(\langle n \rangle - 1)$ is approximately constant ($\sim 0.59$) as predicted by Wroblewski.[6] The ratios of the $q$th moments divided by the $q$th power of the mean multiplicity, i.e., $\langle n^q \rangle / \langle n \rangle^q$, also appear to change slowly in this energy range (not shown). Taken together these results indicate that while exact Koba-Nielsen-Olesen scaling does not hold in this energy regime, it may be approached asymptotically (the Wroblewski formula deviates from exact Koba-Nielsen-Olesen scaling by a term which goes to zero as $1/\langle n \rangle$).[6]

We thank the members of the NAL neutrino laboratory for their aid in the taking of the exposures, and we thank our scanning and measuring personnel for their diligence.

*Research supported by the U.S. Atomic Energy Commission. Computing funds at the University of Rochester are provided by the University.

†Present address: Nevis Laboratories, Columbia University, Irvington-on-Hudson, New York, N. Y. 10533.

‡Alfred P. Sloan Fellow.

[1]J. Chapman *et al.*, Phys. Rev. Lett. 29, 1686 (1972).

[2]The $\pi^0$ spectrum was obtained using $\gamma$ rays converting in the bubble chamber. See A. Seidl *et al.*, University of Michigan Report No. UMBC-7320 and University of Rochester Report No. UR-457 (to be published). 457 (to be published).

[3]The real part of the forward elastic-scattering amplitude is small and does not significantly affect Eq. (2); V. Bartenev *et al.*, Phys. Rev. Lett. 29, 1755 (1972), and private communication from the authors. See also the intersecting-storage-ring data summarized by U. Amaldi, in Proceedings of the Second International Conference on Elementary Particles, Aix-en-Provence, France, September 1973 (to be published).

[4]The 50- and 69-GeV/$c$ data are from V. V. Ammosov *et al.*, Phys. Lett. 42B, 519 (1972); the 205-GeV/$c$ data, G. Charlton *et al.*, Phys. Rev. Lett. 29, 515 (1972); the 303-GeV/$c$ data, NAL Report No. NAL 73/38 and University of California at Los Angeles Report No. UCLA-1077 (to be published).

[5]The $f_2$ moment is defined as $f_2 = \langle n^2 \rangle - \langle n \rangle^2 - \langle n \rangle$; for the other moments see A. H. Mueller, Phys. Rev. D 4, 150 (1971).

[6]Z. Koba, H. B. Nielsen, and P. Olesen, Nucl. Phys. B40, 317 (1970). Also see the analyses given by P. Slattery, Phys. Rev. Lett. 29, 1624 (1972), and Phys. Rev. D 7, 2073 (1973); and by A. Wroblewski, in Lectures at the Thirteenth Cracow School of Theoretical Physics, Cracow, Poland, 1973 (to be published). We stress the importance of the new data at 405 GeV/$c$ and the latest 303- and 50-GeV/$c$ results in reaching these conclusions.